JACS
JOURNAL OF THE AMERICAN CHEMICAL SOCIETY

ARTICLE

pubs.acs.org/JACS

Zirconium-Catalyzed Carboalumination of α-Olefins and Chain Growth of Aluminum Alkyls: Kinetics and Mechanism

James M. Camara,[‡] Robby A. Petros,[§] and Jack R. Norton*[,†]

[†]Department of Chemistry, Columbia University, New York, New York 10027, United States

[‡]Department of Chemistry, University of Illinois at Urbana−Champaign, Urbana, Illinois 61801, United States

[§]Department of Chemistry, University of North Texas, Denton, Texas 76203, United States

Supporting Information

ABSTRACT: A mechanism based on Michaelis−Menten kinetics with competitive inhibition is proposed for both the Zr-catalyzed carboalumination of α-olefins and the Zr-catalyzed chain growth of aluminum alkyls from ethylene. $AlMe_3$ binds to the active catalyst in a rapidly maintained equilibrium to form a Zr/Al heterobimetallic, which inhibits polymerization and transfers chains from Zr to Al. The kinetics of both carboalumination and chain growth have been studied when catalyzed by $[(EBI)Zr(\mu\text{-}Me)_2AlMe_2][B(C_6F_5)_4]$. In accord with the proposed mechanism, both reactions are first-order in [olefin] and [catalyst] and inverse first-order in $[AlR_3]$. The position of the equilibria between various Zr/Al heterobimetallics and the corresponding zirconium methyl cations has been quantified by use of a Dixon plot, yielding $K = 1.1(3) \times 10^{-4}$ M, $4.7(5) \times 10^{-4}$ M, and $7.6(7) \times 10^{-4}$ M at 40 °C in benzene for the catalyst species $[rac\text{-}(EBI)Zr(\mu\text{-}Me)_2AlMe_2][B(C_6F_5)_4]$, $[Cp_2Zr(\mu\text{-}Me)_2AlMe_2][B(C_6F_5)_4]$, and $[Me_2C(Cp)_2Zr(\mu\text{-}Me)_2AlMe_2][B(C_6F_5)_4]$ respectively. These equilibrium constants are consistent with the solution behavior observed for the $[Cp_2Zr(\mu\text{-}Me)_2AlMe_2][B(C_6F_5)_4]$ system, where all relevant species are observable by ^1H NMR. Alternative mechanisms for the Zr-catalyzed carboalumination of olefins involving singly bridged Zr/Al adducts have been discounted on the basis of kinetics and/or ^1H NMR EXSY experiments.

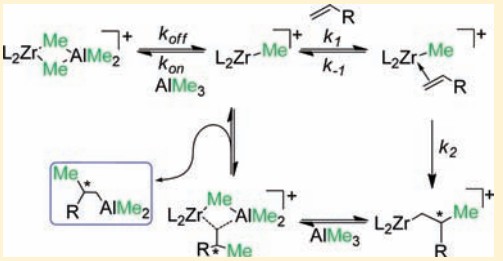

INTRODUCTION

The carbometalation of olefins (eq 1) has found many uses in synthesis.[1] The carboalumination of α-olefins offers particular potential because the product aluminum alkyl may, in principle, be used to prepare alcohols, aldehydes, carboxylic acids, and amidines (Figure 1).[2]

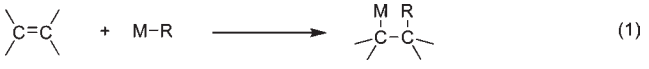

(1)

Dzhemilev and co-workers reported the first zirconium-catalyzed carboalumination in 1985, using $Cp_2ZrCl_2/MgEt_2$ to catalyze the addition of $AlEt_3$ across 1-hexene.[3] Negishi reported a system for the asymmetric carboalumination of α-olefins using bis(1-neomenthylindene)zirconium dichloride[4] as a catalyst and has applied the methodology to natural product synthesis.[5]

Carboalumination reactions play an important role in an industrial setting. The direct carboalumination of ethylene is used in the production of fatty alcohols (linear alcohols with chain lengths between C_6 and C_{22}), also known as Ziegler alcohols. In the Alfol process multiple ethylenes are inserted into the Al−C bonds of triethylaluminum at high temperature and pressure; in the Epal process fewer ethylenes are inserted in each of several short cycles.[6] Oxidation and hydrolysis convert the elongated chains into linear alcohols.

Several groups have explored the catalysis of chain growth in main group organometallics. In 1991, Samsel showed that chain growth in organoaluminums could be catalyzed by Zr and Hf complexes[7] and subsequently reported the catalysis of the same reaction by $Cp^*_2ThCl_2$.[8] Bazan reported the use of $Cp^*CrMe_2(PMe_3)$ to catalyze the insertion of ethylene into Al−C bonds,[9] and Gabbaï demonstrated that $Cp^*Cr(C_6F_5)R$ complexes could catalyze the same reaction.[10] Chen has used a Cp^*ZrCl_2/MAO system[11] and Kempe has used an organoyttrium/AlR_3 system[12] to produce polyethylene with low polydispersity. Gibson has shown that a bis(imino)pyridine iron complex can catalyze the insertion of ethylene into Zn−C bonds and has established that Fe/Zn transfer is fast and reversible throughout such a polymerization ("catalyzed chain growth").[13] Fast and reversible transfers among an organozinc compound, a Zr catalyst, and an Hf catalyst have been used to effect "chain shuttling", producing block copolymers with different levels of α-olefin incorporation.[14] Recently, Sita and co-workers have described the use of a Hf catalyst to effect the apparent chain growth of aluminum alkyl chains; insertion of ethyene into Hf−C bonds is followed by chain transfer to Al through ZnR_2.[15]

The exchange of alkyl chains between Zr and Al surely occurs via the formation of a Zr/Al bimetallic complex like **1**, first reported by Bochmann and Lancaster.[16] We have previously reported[17] the

Received: May 11, 2010
Published: March 23, 2011

dx.doi.org/10.1021/ja104032w | J. Am. Chem. Soc. 2011, 133, 5263–5273

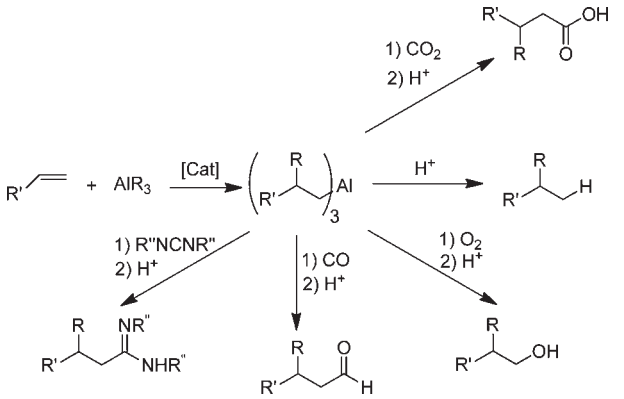

Figure 1. Potential transformations of aluminum alkyls.

rate constant k_{off} for the exchange of $AlMe_3$ from **1** (and other such complexes) into $(AlMe_3)_2$ in C_6D_6, presumably by dissociation as in reaction 2. Both cations in eq 2 are solvated to some extent by the aromatics (bezene, toluene) in which carboalumination and chain growth are usually carried out.

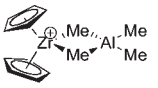

1

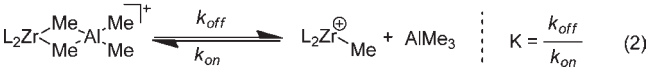

$$K = \frac{k_{off}}{k_{on}} \qquad (2)$$

Other researchers have observed species similar to **1** and have suggested that they are involved in chain transfer.[18] The X-ray structure of the related complex $[Ti(N^tBu)(Me_3[9]aneN_3)(\mu\text{-}Me)_2AlMe_2]^+$ has been published, along with the results of calculations on such methyl-bridged heterobimetallics.[19]

The mechanism by which Zr catalyzes the carboalumination in eq 3 has been examined by Shaughnessy and Waymouth.[20] Their study yielded surprising results, with the reaction appearing to be first-order in substrate (allylbenzene) but second-order in the zirconium catalyst and of variable order in $AlMe_3$ (−2 at $[AlMe_3]$ between 0.64 and 1.27 M, −0.75 at $[AlMe_3] > 1.27$ M). However, the concentrations of $AlMe_3$ used were sufficiently small that $[AlMe_3]$ varied during the reactions. Furthermore, experiments in our laboratories have shown that Me/C_6F_5 exchange between Al and B is facile under the conditions of reaction 3 and have identified BMe_3 as a product.[17] (The reported synthesis of $Al(C_6F_5)_3$ involves the reaction of $B(C_6F_5)_3$ and $AlMe_3$.[21]) Moreover, the use of $B(C_6F_5)_3$ as an activator is known to produce a tight ion pair,[22] complicating the reaction kinetics.

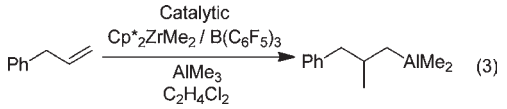

(3)

We have therefore examined the kinetics and mechanism of the carboalumination in eq 4 (L_2 = EBI, Cp_2, and $Me_2C(C_5H_4)_2$) and of the AlR_3 chain growth in eq 5. To generate the catalysts we have treated the appropriate dimethyl metallocene with $[Ph_3C][B(C_6F_5)_4]$ ($B(C_6F_5)_4^-$ is known to be weakly coordinating).[23] We have already shown that activation by this reagent forms Cp_2ZrMe^+ from Cp_2ZrMe_2 without Me/C_6F_5 exchange (the only side product is triphenylethane)[17] and that

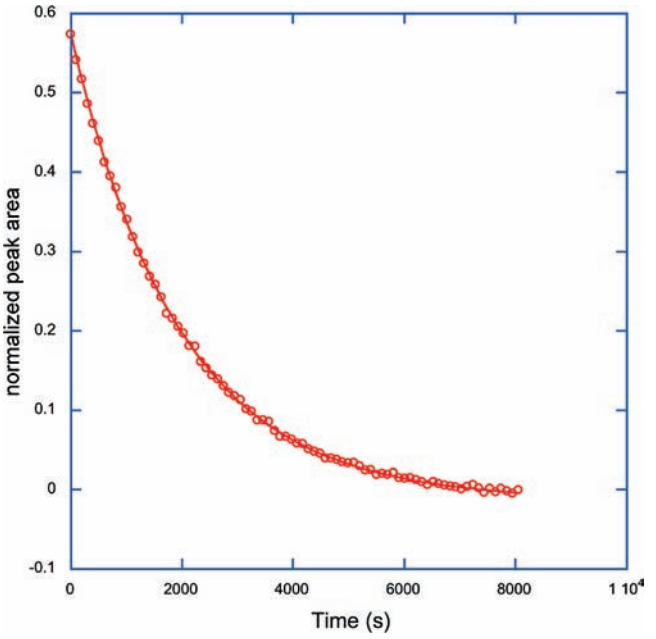

Figure 2. First-order exponential fit to the disappearance of allylbenzene during methylalumination in the presence of $[(EBI)Zr(\mu\text{-}Me)_2AlMe_2][B(C_6F_5)_4]$ (eq 4) at 40 °C in C_6D_6. $[(EBI)Zr(\mu\text{-}Me)_2AlMe_2]^+$ = 0.38 mM, $[allylbenzene]_o$ = 2.55 mM, $[AlMe_3]_{total}$ = 61.2 mM.

it may be used to form the known[18g] heterobimetallic cation $[(EBI)Zr(\mu\text{-}Me)_2AlMe_2]^+$ (**3**) cleanly from $(EBI)ZrMe_2$ in the presence of excess $(AlMe_3)_2$ as in eq 6.[24]

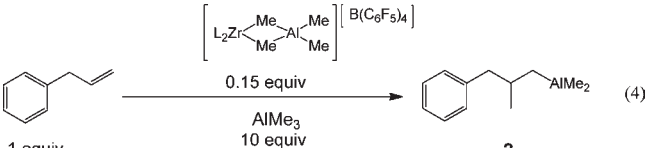

(4)

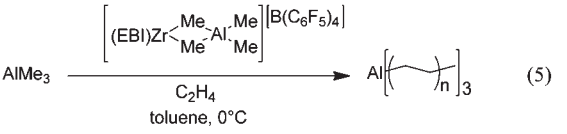

(5)

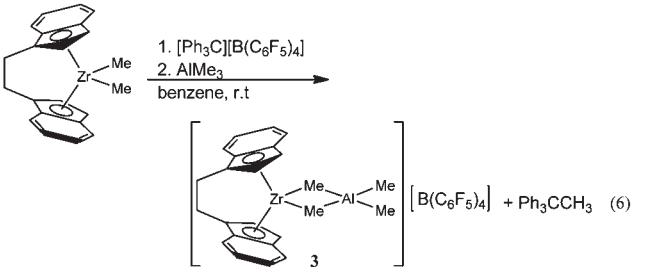

(6)

RESULTS AND DISCUSSION

Kinetics of Zr-Catalyzed Carboalumination (reaction 4). The dimethyl metallocene precatalyst (e.g., $(EBI)ZrMe_2$) was

dx.doi.org/10.1021/ja104032w | J. Am. Chem. Soc. 2011, 133, 5263–5273

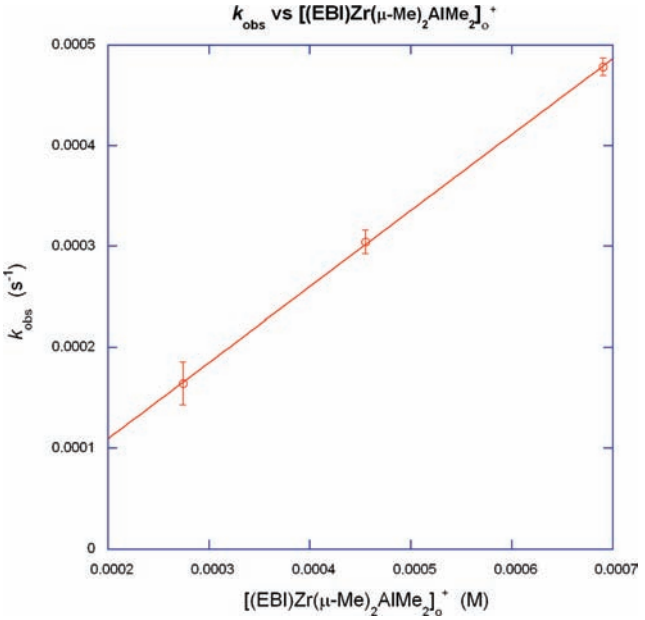

Figure 3. Plot of k_{obs} (reaction 4) for disappearance of allylbenzene at 40 °C in C_6D_6 vs $[(EBI)Zr(\mu\text{-}Me)_2AlMe_2]^+$ initially added. $[allylbenzene]_o$ = 6.12 mM, $[AlMe_3]_{total}$ = 61.2 mM.

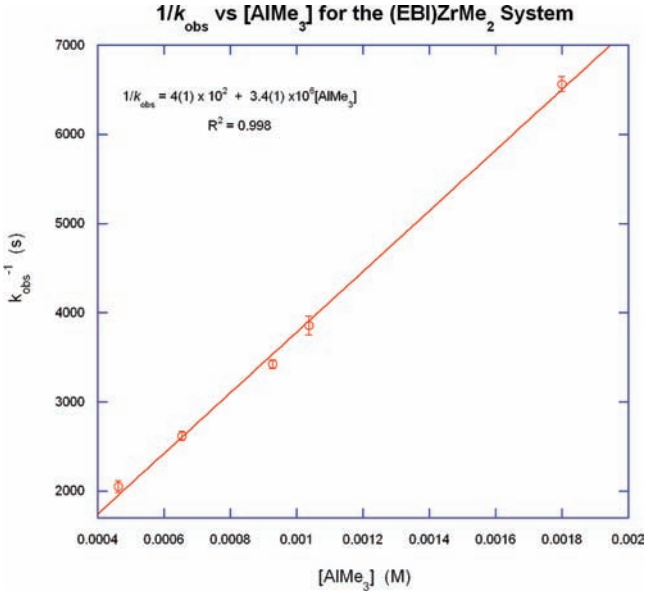

Figure 4. Plot of k_{obs}^{-1} (s) (reaction 4) measured under pseudo-first-order conditions vs $[AlMe_3]$ in mol/L. $[(EBI)Zr(\mu\text{-}Me)_2AlMe_2]^+$ = 0.38 mM, $[allylbenzene]_o$ = 2.55 mM, T = 40 °C.

activated with 1 equiv of $[Ph_3C][B(C_6F_5)_4]$ in benzene and converted to the heterobimetallic (e.g., **3**) by addition of >2 equiv[25] of $(AlMe_3)_2$. The disappearance of allylbenzene was monitored at 40 °C in C_6D_6 in the presence of 0.15 equiv of catalyst and a substantial excess (10 equiv) of $(AlMe_3)_2$. We saw no oligomerization. ^{1}H NMR (stack plot in Figure S-1) showed that the allylbenzene was converted cleanly to the product **2**. The disappearance of the allylbenzene was cleanly first-order, k_{obs} = 5.1×10^{-4} s^{-1} (Figure 2).

A plot of k_{obs} against the amount of $[(EBI)Zr(\mu\text{-}Me)_2AlMe_2]^+$ initially added gave Figure 3. (The data are in Table S-1.) Reaction 4 is thus *first-order* in Zr.

Probing the order in $AlMe_3$ proved more challenging. Trimethylaluminum exists mostly as the dimer $(AlMe_3)_2$ under the reaction conditions (40 °C in C_6D_6). The equilibrium constant K_{TMA} (eq 7) can be estimated from published data for the dissociation of $(AlMe_3)_2$ in mesitylene. Cerny and co-workers have reported ΔH = 13.1(8) kcal/mol and ΔS = 19(2) cal/(mol·K),[26] which imply a ΔG of 7.1 kcal/mol at 40 °C and a K_{TMA} of 1.2×10^{-5} M at that temperature.

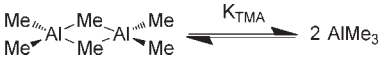

(7)

Noting that the equilibrium in eq 7 is rapidly maintained on the time scale of the carboalumination reaction,[26] and assuming that the above value of K_{TMA} is valid in benzene, the amount of monomeric $AlMe_3$ may be calculated from the total amount of added trimethylaluminum. Measurements of k_{obs} with various amounts of added trimethylaluminum (but at least a 10-fold excess over the allylbenzene substrate) gave the results in Table S-2. Comparison of k_{obs} (for eq 4) with $[AlMe_3]$ suggested a rate law inverse in $AlMe_3$, and a plot of $1/k_{obs}$ vs $[AlMe_3]$ proved linear (Figure 4).

The rate law for our carboalumination (reaction 4) is thus first-order in substrate and [Zr] and inverse first-order in $[AlMe_3]$:

$$\text{rate} = k_{obs}\frac{[\text{allylbenzene}][\text{Zr}]}{[AlMe_3]} \qquad (8)$$

Mechanism of Zr-Catalyzed Carboalumination. The mechanism in Scheme 1 is consistent with our observed rate law (eq 8). A reactive zirconium methyl cation **B** reversibly binds $AlMe_3$ to form an inactive Zr/Al heterobimetallic **A**.[27] The cation **B** coordinates the olefin with rate constant k_1, forming **C**; **C** inserts the olefin with rate constant k_2, forming a longer-chain alkyl Zr cation. That cation then reassociates with free $AlMe_3$ to form a new heterobimetallic **A′**, resulting in transmetalation and formation of the product **P** when **A′** dissociates in the direction shown.

Deriving the rate law for this mechanism is straightforward. If the formation of **A′** and loss of **P** are faster than chain growth, the rate of formation of **P** is given by eq 9. The concentration of **C** (which is not observable) is surely small enough to justify the steady-state approximation, which gives eq 10.

$$\frac{dP}{dt} = k_2[\mathbf{C}] \qquad (9)$$

$$\frac{d[\mathbf{P}]}{dt} = \frac{k_2k_1[\text{olefin}][\mathbf{B}]}{k_{-1}+k_2} \qquad (10)$$

As the $AlMe_3$-binding equilibrium (eqs 2 and 11) is rapidly maintained on the carboalumination time scale,[17] we can express [**B**] as a function of the total zirconium concentration $[Zr]_T$, [olefin], and $[AlMe_3]$ (eq 12).

$$K = \frac{k_{off}}{k_{on}} = \frac{[AlMe_3][\mathbf{B}]}{\mathbf{A}} \Rightarrow [\mathbf{A}] = \frac{[AlMe_3][\mathbf{B}]}{\mathrm{K}} \qquad (11)$$

dx.doi.org/10.1021/ja104032w |J. Am. Chem. Soc. 2011, 133, 5263–5273

Scheme 1. Proposed Mechanism for the Zr-Catalyzed Carboalumination of α-Olefins (L_2 = EBI, Cp_2, or $Me_2C(C_5H_4)_2$)

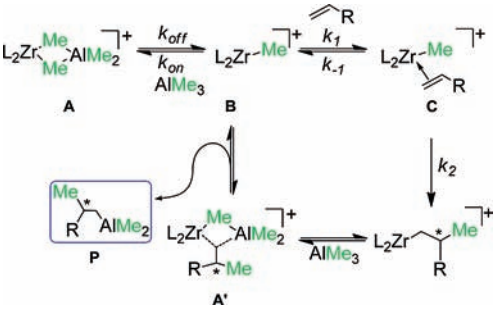

Scheme 2. Michaelis–Menten Kinetics with Competitive Inhibition

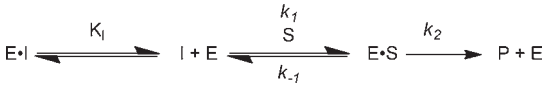

Table 1. Comparison of k_{off} Values (eq 2, 27 °C) with Dissociation Equilibrium Constants K (40 °C) in C_6D_6

	k_{off} (s^{-1})	$K = k_{off}/k_{on}$ (M)
$[(EBI)Zr(\mu\text{-}Me)_2AlMe_2]^+$ (**3**)	0.2(1)	$1.1(3) \times 10^{-4}$
$[Cp_2Zr(\mu\text{-}Me)_2]AlMe_2]^+$ (**1**)	0.12(1)	$4.7(5) \times 10^{-4}$
$[Me_2C(C_5H_4)_2Zr](\mu\text{-}Me)_2]AlMe_2]^+$ (**4**)	1.8(1)	$7.6(7) \times 10^{-4}$

$$[\mathbf{B}] = \frac{[\mathrm{Zr}]_T}{\frac{[\mathrm{AlMe_3}]}{K} + 1 + \frac{k_1[\mathrm{olefin}]}{k_{-1}+k_2}} \quad (12)$$

Substitution of eq 12 into eq 10 gives eq 13.

$$\frac{d[\mathbf{P}]}{dt} = \frac{k_2[\mathrm{olefin}][\mathrm{Zr}]_T}{\left(\frac{k_{-1}+k_2}{k_1}\right)\left(\frac{[\mathrm{AlMe_3}]}{K}+1\right) + [\mathrm{olefin}]} \quad (13)$$

If $k_2 \gg k_1$ and the accumulation of **C** is negligible, the last term disappears from the denominator and we obtain a rate law, eq 14, that is consistent with our kinetic observations.

$$\frac{d[\mathbf{P}]}{dt} = \frac{k_2[\mathrm{olefin}][\mathrm{Zr}]_T}{\left(\frac{k_{-1}+k_2}{k_1}\right)\left(\frac{[\mathrm{AlMe_3}]}{K}+1\right)} \quad (14)$$

Scheme 1 is analogous to the competitive inhibition of the Michaelis–Menten situation in Scheme 2, which gives the familiar rate law[28] in eq 15; a negligible accumulation of **E•S** reduces that rate law to eq 16.

$$\frac{d[\mathbf{P}]}{dt} = \frac{k_2[\mathbf{S}][\mathbf{E}]_T}{\left(\frac{k_{-1}+k_2}{k_1}\right)\left(\frac{[\mathbf{I}]}{K_1}+1\right) + [\mathbf{S}]} \quad (15)$$

$$\frac{d[\mathbf{P}]}{dt} = \frac{k_2[\mathbf{S}][\mathbf{E}]_T}{\left(\frac{k_{-1}+k_2}{k_1}\right)\left(\frac{[\mathbf{I}]}{K_1}+1\right)} \quad (16)$$

The rate laws in eqs 14 and 16 are the same. In eq 14 the zirconium alkyl cation **B** is the "enzyme", the Zr/Al heterobimetallic **A** is the "enzyme–inhibitor complex", and the olefin is the "substrate", **S**. The only significant difference between Schemes 1 and 2 is the fact that AlR_3 is both an inhibitor and a reactant in Scheme 1. This does not affect the rate law because AlR_3 serves as a reactant only after the rate-determining step.

Determination of Equilibrium Constants *K* for the Dissociation of $AlMe_3$ from Zr/Al Heterobimetallic Cations. Plots like those in Figure 4 allow for the determination of the equilibrium constant K (eq 2). From eq 14, k_{obs} for the disappearance of allylbenzene will be given by eq 17, and inversion of eq 17 gives the expression in eq 18. From eq 18, it is clear that a plot of $1/k_{obs}$ vs $[AlMe_3]$ should be a straight line (analogous to a Dixon plot), as observed in Figure 4. Dividing its intercept by its slope will give the equilibrium constant K (eq 19).

$$k_{obs} = \frac{k_2[\mathrm{Zr}]_T}{\frac{k_{-1}+k_2}{k_1}\left(\frac{[\mathrm{AlMe_3}]}{K}+1\right)} \quad (17)$$

$$\frac{1}{k_{obs}} = \frac{(k_{-1}+k_2)}{Kk_1k_2[\mathrm{Zr}]_T}[\mathrm{AlMe_3}] + \frac{(k_{-1}+k_2)}{k_1k_2[\mathrm{Zr}]_T} \quad (18)$$

$$\frac{\text{intercept}}{\text{slope}} = \frac{\frac{(k_{-1}+k_2)}{k_1k_2[\mathrm{Zr}]_T}}{\frac{(k_{-1}+k_2)}{Kk_1k_2[\mathrm{Zr}]_T}} = K \quad (19)$$

The intercept and slope of the plot in Figure 4 imply[29] that K for the EBI heterobimetallic **3** is $1.1(3) \times 10^{-4}$ M in benzene at 40 °C. Similar experiments (the reagent concentrations and the resulting k_{obs} values are in Table S-2) with the unbridged Cp_2 Zr/Al (**1**) and the Me_2C-bridged Zr/Al (**4**) give the other K values in Table 1.

Our previously measured[17] values of k_{off} at 27 °C (also in benzene) are given in Table 1 for comparison.[30,31] While **4** shows both a relatively large k_{off} and a relatively large K, the relationship between k_{off} and K is not in general linear; i.e., k_{on} is not constant from one zirconocene to another.

Olefin and Catalyst Dependence of the Zr-Catalyzed Growth of Organoaluminum Chains (eq 5). Determining the rate law for such a reaction is challenging. Use of ethylene requires a pressure vessel. Zirconium methyl cations are highly active catalysts, and chain growth may become limited by mass transport; rate measurements will not be informative unless the reaction is slower than the rate at which the ethylene dissolves. The growth reaction is exothermic making temperature control difficult. Finally, the growth of the chains during the reaction leads to an increase in the viscosity of the solution, which affects the rate of further chain growth.

The apparatus in Figure 5 enabled us to monitor ethylene uptake as a function of time (details in Supporting Information). A flow meter calibrated for ethylene was connected to a mass totalizer, which recorded the total amount of ethylene that had been admitted to the system as a function of time. The ethylene passed through copper cooling coils into a multiport pressure vessel with a thermocouple, pressure gauge, pressure relief valve, injection port, and mechanical stirrer. The vessel was immersed as completely as possible in a 0 °C cold bath, which required that

dx.doi.org/10.1021/ja104032w | J. Am. Chem. Soc. 2011, 133, 5263–5273

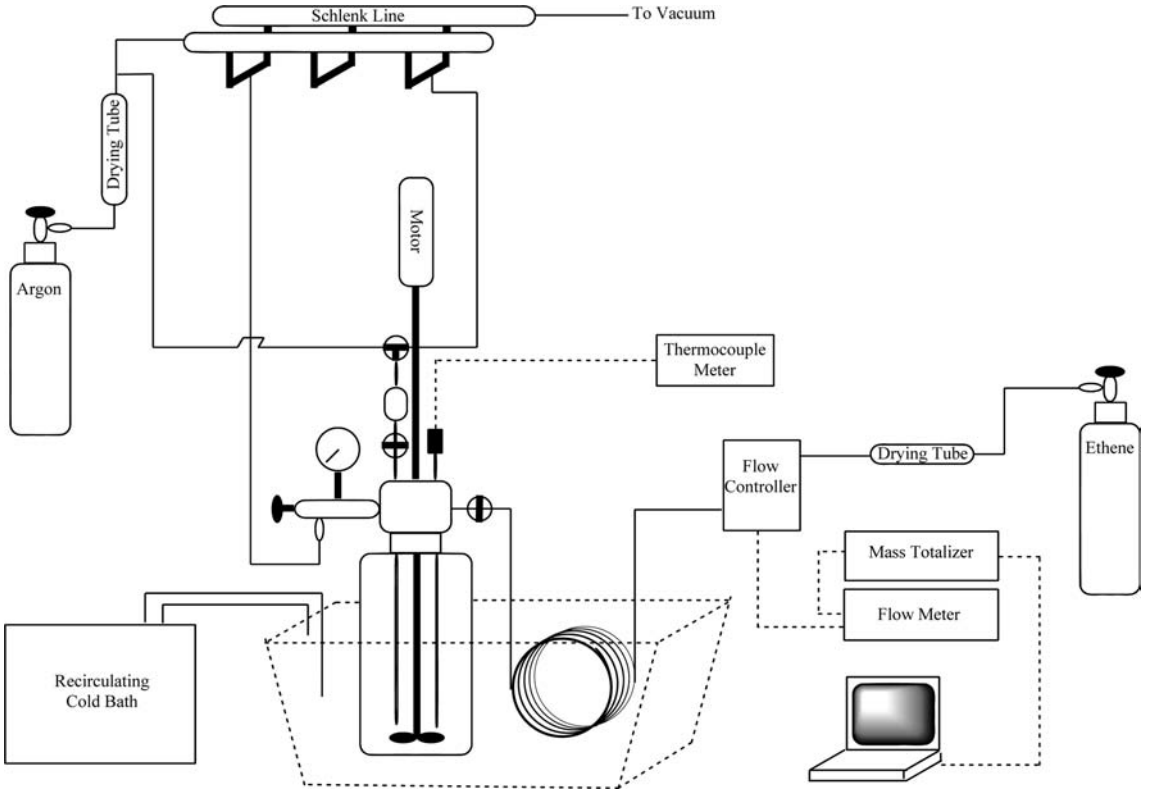

Figure 5. Diagram of the reactor used for measuring chain growth kinetics.

the benzene used as solvent in our carboalumination studies be replaced with toluene. The reaction proved sufficiently exothermic that its temperature rose slightly above that of the bath, being about 1.5 ± 0.5 °C during data collection.

The precatalyst (EBI)$ZrMe_2$ was again activated with 1 equiv of $[Ph_3C][B(C_6F_5)_4]$ and converted to the heterobimetallic **2** by addition of >2 equiv of $(AlMe_3)_2$. Admitting ethylene (20 psig) to the evacuated reaction gave uptake plots like that in Figure 6. Initial fast absorption as the reaction vessel filled and ethylene dissolved in the toluene gave way to a modest but constant slope after the solution had become saturated with ethylene. This slope, due to chain growth, gave the rate of the reaction. It was unaffected by a change in the stirring speed, verifying that the rate was not limited by mass transport.

The concentrations of ethylene at various pressures were determined from ethylene uptake measurements on pure toluene (Table 2). The results were consistent with those reported by other researchers.[32]

Our kinetics experiments at ethylene pressures >40 psig showed chain growth to be so fast that it became limited by mass transport. At ethylene pressures <20 psig the reaction was so slow that the mass totalizer did not give reliable readings. Within that pressure range (20 to 40 psig), however, the rate of chain growth appeared to be linear with $[C_2H_4]$ (Table S-3 and Figure S-2). At 20 psig ethylene, variation of $[Zr]_{tot}$ showed the rate of chain growth to be linear in catalyst (Table S-4 and Figure S-3).

Products from Zr-Catalyzed Growth of Organoaluminum Chains (eq 5) and Estimation of Monomeric AlR_3. Hydrolysis of the organoaluminum products from a typical experiment (20 psig ethylene, 4.39 μM catalyst, 439 mM $AlMe_3$, 6 min reaction time) resulted in considerable gas evolution, implying that many Al−Me bonds remained unchanged after ethylene uptake.

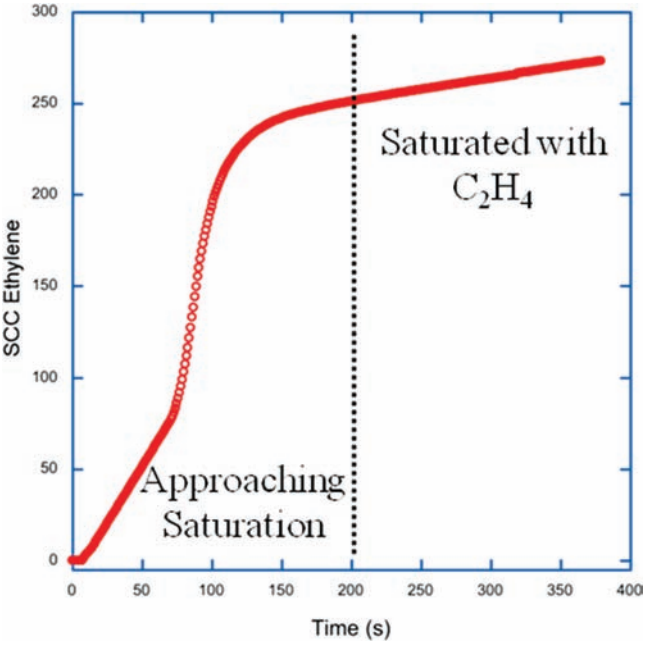

Figure 6. Typical ethylene uptake curve obtained from the reactor for a catalyzed chain growth reaction (T = 0 °C, $P_{ethylene}$ = 20 psig, [(EBI)Zr-(μ-Me)$_2$$AlMe_2$]$^+$ = 4.39 μM, [$AlMe_3$] = 0.439 M).

Considerable polymer (~150 mg) precipitated, which GPC showed to have an M_w of 92 000, an M_n of 29 000, and a PDI of 3.2 (Figure S-4). ^{1}H NMR showed the polymer to contain almost no unsaturation (Figure S-5). If the organoaluminum products were exposed to O_2 before hydrolysis, no gas was evolved.

dx.doi.org/10.1021/ja104032w |*J. Am. Chem. Soc.* 2011, 133, 5263–5273

Table 2. Solubility of Ethylene in Toluene at 0 °C Measured at Various Pressures

Pressure (psig)	[Ethylene] (M)
20	0.44
30	0.59
40	0.79

Table 3. Equilibrium Constants for Dissociation of $(AlR_3)_2$ for Various Trialkylaluminums at 50 °C in Benzene[33]

AlR_3	K_{Al}
$AlMe_3$	7.4×10^{-7}
$AlEt_3$	1.4×10^{-4}
$Al(n\text{-}Pr)_3$	2.5×10^{-3}
$Al(n\text{-}Bu)_3$	5.0×10^{-3}
$Al(n\text{-}Hep)_3$	7.1×10^{-3}
$Al(n\text{-}Oct)_3$	8.2×10^{-3}
$Al(n\text{-}Dec)_3$	9.1×10^{-3}
$Al(i\text{-}Bu)_3$	6.0

The distribution of chain lengths implied by these results made it difficult to quantify the monomeric AlR_3 that was inhibiting ethylene uptake. The rates were typically measured >200 s after the reaction was initiated, by which time there had been significant ethylene uptake. Some idea of the effect of chain length on association can be obtained from the reported equilibrium constants K_{Al} (for dissociation of AlR_3 dimers) in Table 3. The values of K_{Al} are not significantly affected by chain length past butyl, although they are affected by chain branching.

In order to determine how many Al−C bonds inserted ethylene during a typical reaction and what portion of the ethylene became polymer, we performed the following experiment. A chain growth reaction was conducted under typical reaction conditions (20 psig ethylene, 4.39 μM catalyst, 439 mM $AlMe_3$), with the ethylene flow restricted to no more than 300 SCC/min by the flow controller; under these conditions we could measure accurately the consumption of ethylene throughout the reaction.[34] The reaction time was extended to 8 min to ensure that the solution had become saturated before rate measurement; the rate of ethylene uptake after saturation was the same as that observed in previous experiments with the same Zr, Al, and C_2H_4 concentrations. A total of 108 SCC of ethylene (~123 mg, or 4.4 mmol) was consumed during this time (Figure S-9).

After quenching and hydrolysis, polymer (106 mg) again precipitated, containing *~85% of the ethylene consumed*. The organic layer was separated, neutralized, dried, and analyzed by ^{1}H NMR and MS. Its ^{1}H NMR showed the presence of oligomeric material, as evidenced by the ratio of methylene H's to methyl H's (≈ 13:1). The polymer was analyzed by GPC and found to have M_n = 67 500, M_w = 172 500, and PDI = 2.56. Analysis of the polymer by ^{1}H NMR showed almost no unsaturation, implying that chain transfer to aluminum was the principal termination mechanism. In view of the length of the polymer chains, and the small number of ethylenes consumed per Al (4.4 mmol ethylene per 43.9 mmol of Al), it was apparent that *chain growth had occurred in only a small portion of the $AlMe_3$*.

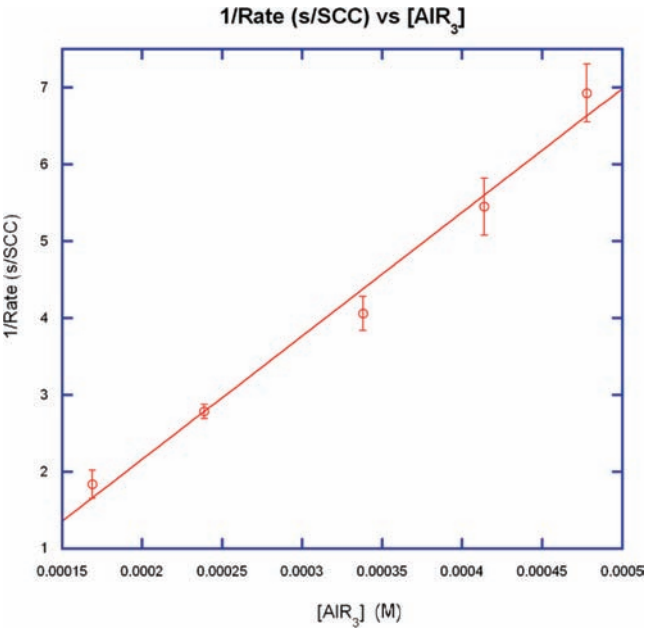

Figure 7. Dependence of Zr-catalyzed chain growth on $[AlR_3]$ (eq 5). $[AlR_3]$ was calculated from the equilibrium constant for dissociation of trimethylaluminum[26] at 0 °C in mesitylene ($P_{ethylene}$ = 20 psig, $[(EBI)\text{-}Zr(\mu\text{-}Me)_2AlMe_2]^+$ = 4.39 μM).

Chain growth experiments were conducted with $Al(oct)_3$ in place of $AlMe_3$. In this system, the shortest chain produced upon hydrolysis would be nonvolatile C_8. A plot of total ethylene uptake vs time implied a rate of 0.18 SCC/s, only slightly greater than the rates determined for the same experiment with $AlMe_3$. Hydrolysis of the products from a quenched reaction under typical conditions (20 psig ethylene, 439 mM Al, 4.39 μM catalyst) produced *only* polymer and octane. The absence of any detectable short oligomers suggests that $Al(oct)_3$ is a less effective inhibitor of catalysis than $AlMe_3$—not surprising in view of the decrease in K_{Al} from trioctylaluminum to trimethylaluminum (Table 3). Importantly, these data verify that polymer is the principal product from chain growth.

In chain growth experiments beginning with trimethylaluminum, unreacted *$AlMe_3$ and its dimer remain the predominant organoaluminum species throughout the experiment*. Thus, the concentration of inhibiting monomeric AlR_3 in an experiment can be estimated from K_{Al} for $AlMe_3$ and the amount of trimethylaluminum initially added. The data (Table S-3) show that the rate of chain growth declines with increasing $[AlMe_3]$, and a plot of 1/rate vs $[AlR_3]$ is linear (Figure 7). To ensure that this observation is not coincidental with our choice of K_{Al}, we have also estimated the concentration of monomeric AlR_3 from K_{Al} for trioctylaluminum (Figure S-10);[33d] the plot of 1/rate vs $[AlR_3]$ is still linear. The growth of our organoaluminum chains (reaction 5) thus obeys a rate law like the one (eq 8) that we established for carboalumination (reaction 4).

The agreement of the observed rate law for chain growth with that of carboalumination suggests that chain growth occurs by a mechanism (Scheme 3) like the one in Scheme 1 for carboalumination. A kinetic analysis like that for Scheme 1 gives the rate law in eq 20 from Scheme 3. If the olefin complex **C** does not accumulate, eq 20 reduces to eq 21 (just as eq 13 reduced to eq 14 for Scheme 1). Inversion of eq 21 gives eq 22, which shows

Scheme 3. Zirconium-Catalyzed Chain Growth of Aluminum Alkyls[a]

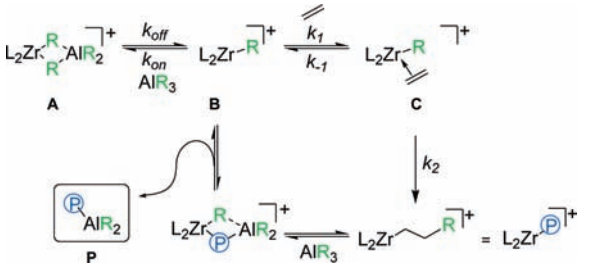

[a] At short reaction times R = Me, at longer reaction times R = P.

that a plot of 1/rate vs $[AlR_3]$ should be linear.

$$\frac{d[\mathbf{P}]}{dt} = \frac{k_2[\text{olefin}][\text{Zr}]_T}{\left(\frac{k_{-1}+k_2}{k_1}\right)\left(\frac{[AlR_3]}{K}+1\right)+[\text{olefin}]} \quad (20)$$

$$\text{if } [\text{olefin}] \ll \left(\frac{k_{-1}+k_2}{k_1}\right)\left(\frac{[AlR_3]}{K}+1\right) \text{ then}$$

$$\frac{d[\mathbf{P}]}{dt} = \frac{k_2[\text{olefin}][\text{Zr}]_T}{\left(\frac{k_{-1}+k_2}{k_1}\right)\left(\frac{[AlR_3]}{K}+1\right)} \quad (21)$$

$$\frac{1}{\frac{d[\mathbf{P}]}{dt}} = \frac{\left(\frac{k_{-1}+k_2}{k_1}\right)\left(\frac{[AlR_3]}{K}+1\right)}{k_2[\text{olefin}][\text{Zr}]_T} = \frac{(k_{-1}+k_2)}{Kk_1k_2[\text{Zr}]_T}[AlMe_3] + \frac{(k_{-1}+k_2)}{k_1k_2[\text{Zr}]_T} \quad (22)$$

It is, however, not practical to determine the equilibrium constant K (for the dissociation of **3**) from the intercept and slope of the plot in Figure 7. There is not a simple dissociation equilibrium, but rather many dissociation equilibria involving various AlR_3 present. The concentrations of monomeric AlR_3 are only estimates, and the plot in Figure 7 (while linear enough to be consistent with eq 22 and Scheme 3) does not determine the intercept with precision.

Direct Determination of the Dissociation Equilibrium Constants *K* for the Cp Heterobimetallic 1. In principle, the values of K determined by eqs 18 and 19 from carboalumination data can be checked by direct examination of the appropriate dissociation equilibria (eq 2). However, the complexity of their ^{1}H NMR spectra makes it hard to quantify the dissociation of the EBI heterobimetallic **3** or the Me_2C-bridged heterobimetallic **4**.

In contrast the resonances of $[Cp_2ZrMe][B(C_6F_5)_4]$[35] are easily distinguished from the resonances of the Zr/Al heterobimetallic **1**. When $[Cp_2ZrMe][B(C_6F_5)_4]$ was generated from Cp_2ZrMe_2 and $[Ph_3C][B(C_6F_5)_4]$, its ^{1}H NMR spectrum in benzene at 40 °C (Figure S-6) showed *clean conversion to* $[Cp_2ZrMe][B(C_6F_5)_4]$. The addition of exactly 1.0 equiv of trimethylaluminum *did not convert all of the* $[Cp_2ZrMe][B(C_6F_5)_4]$ *to* **1** (Figure S-7), although the conversion became quantitative after the addition of *excess* $AlMe_3$.[36] Stack plots of the ^{1}H NMR spectra taken as $AlMe_3$ was added are shown in Figure S-8.

Scheme 4. Alternative Mechanism for Zr-Catalyzed Carboalumination of Olefins Involving a Singly Bridged, Coordinatively Unsaturated and Catalytically Active Zr/Al Heterobimetallic D (L_2 = Cp_2, SBI, EBI, and similar)

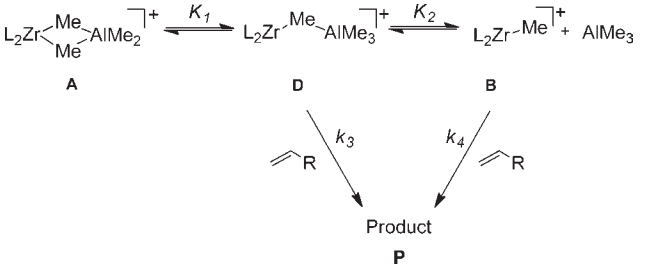

Scheme 5. Exchange of Bridging and Terminal Methyl Groups by Rotation around the Al−C Bond of D

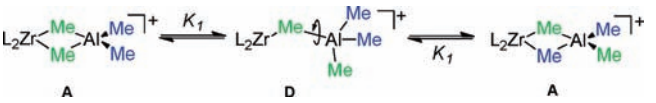

Integration of the spectrum with 1.0 equiv of $AlMe_3$ showed that the residual $[Cp_2ZrMe][B(C_6F_5)_4]$ was ~0.43 mM, in good agreement with the estimated value of 0.5(1) mM calculated from our measurement of K for **1** ($4.7(5) \times 10^{-4}$ M).

Alternatives to Schemes 1 and 3. The alkyl bridges in Schemes 1 and 3 break in a *pairwise* fashion; i.e., the two alkyl bridges in **A** open synchronously to the mononuclear **B** and $AlMe_3$. It is possible that one alkyl bridge opens more rapidly than the other, giving a singly bridged intermediate like **D** in Scheme 4. (For simplicity we write the bridges as methyl groups.) Such an intermediate could coordinate the substrate olefin (rate constant k_3) without further dissociation.

If coordination is rate determining, the rate law derived for this mechanism is given in eq 23. The reciprocal of the corresponding observed pseudo-first-order rate constant is given by eq 24. (Derivations of these equations are given in the Supporting Information.) It is clear that eq 24 is *not* linear in $[AlMe_3]$, so Scheme 4 is inconsistent with our kinetic observations (or at least not supported by them).

$$-\frac{dP}{dt} = \frac{k_3[\text{olefin}][AlMe_3][\text{Zr}]_T}{K_2\left(1+\frac{[AlMe_3]}{K_2}+\frac{[AlMe_3]}{K_1K_2}\right)} + \frac{k_4[\text{olefin}][\text{Zr}]_T}{1+\frac{[AlMe_3]}{K_2}+\frac{[AlMe_3]}{K_1K_2}} \quad (23)$$

$$\frac{1}{k_{obs}} = \frac{K_2\left(1+\frac{[AlMe_3]}{K_2}+\frac{[AlMe_3]}{K_1K_2}\right)}{k_3[AlMe_3][\text{Zr}]_T + K_2k_4[\text{Zr}]_T} \quad (24)$$

If k_3 is negligible, Scheme 4 becomes kinetically equivalent to Schemes 1 and 3. If k_4 is negligible we obtain a derived rate law with k_{obs} given by eq 25, which cannot be linear in $[AlMe_3]$ and is inconsistent with the observed kinetics.

$$\frac{1}{k_{obs}} = \frac{K_2}{k_3[AlMe_3][\text{Zr}]_T} + \frac{1}{k_3[\text{Zr}]_T} + \frac{1}{K_1k_3[\text{Zr}]_T} \quad (25)$$

An even more convincing argument against the presence of a significant amount of a singly bridged Zr/Al species such as **D** is

dx.doi.org/10.1021/ja104032w |J. Am. Chem. Soc. 2011, 133, 5263–5273

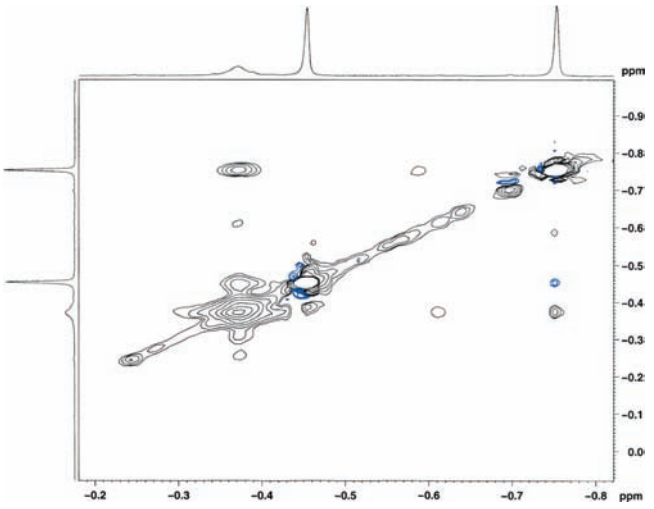

Figure 8. ^{1}H NMR EXSY spectrum of $[Cp_2Zr(\mu\text{-}Me)_2AlMe_2][B(C_6F_5)_4]$ (**1**) in benzene at 40 °C with a mixing time of 300 ms. $AlMe_3$ ($\delta = -0.38$) is seen to exchange with the bridging methyl groups ($\delta = -0.46$) and the terminal methyl groups ($\delta = -0.77$).

offered by the ^{1}H NMR of Zr/Al heterobimetallics. Formation of **D**, and rotation around its Al−C bond, would result in *fast direct exchange* of the terminal and bridging methyl groups (Scheme 5).

Direct exchange of this type should result in readily observable bridge/terminal cross peaks in the ^{1}H NMR EXSY spectrum of solutions of a heterobimetallic **A**. However, no such exchange is seen for **1** in Figure 8. (Variation of mixing time makes no difference.) The bridging methyls and the terminal methyls of **1** do, as we would expect from the operation of the equilibrium in eq 2, *both* exchange with free trimethylaluminum. Trimethylaluminum itself gives similar results: exchange between the bridging and the terminal methyl groups of the dimer $(AlMe_3)_2$ takes place principally by dissociation into the $AlMe_3$ monomer.[26]

The fact that there is no observable direct exchange between the bridging and terminal methyl groups of **A** argues against noncompetitive inhibition,[37] in which the substrate binds to **D** rather than to the Zr methyl cation **B** and forms product at an attenuated rate. While such mechanisms can in principle be tested kinetically, it is not practical in our system[38] to achieve the required range of concentrations of the $AlMe_3$ monomer.

Catalyzed Chain Growth and Catalytic Chain Growth. Gibson and co-workers have distinguished "catalyzed chain growth", with *fast* and *reversible* exchange of the polymer chain between a transition metal and Al, from "catalytic chain growth", in which the transition metal catalyzes olefin insertion and chain growth without implying anything about the *rate* of chain *exchange* between the transition metal and Al.[13a] *Catalyzed* chain growth produces a Poisson distribution of molecular weights; modeling studies[13a] show that the rate of Zr/Al transfer must be at least 100 times faster than the rate of propagation in order to achieve such a distribution.

Our kinetics confirm that AlR_3 monomers bind to the Zr cations in "competitive inhibition" preequilibria but reveal nothing about how rapidly chains are exchanged between Zr and Al. However, most of the product in our experiments is polyethylene of high polydispersity, implying that insertion into Zr−C is much faster than chain transfer from Zr to Al. Thus, our chain growths *are not* "catalyzed chain growth reactions" as defined by Gibson and co-workers.[13a]

Scheme 6. Fast Insertion Relative to Coordination of Olefin to Zirconium Alkyl Cation

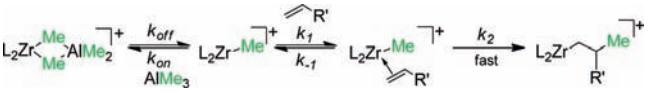

Scheme 7. Rapid Unfavorable Binding of Olefin Followed by Rate-Determining Insertion

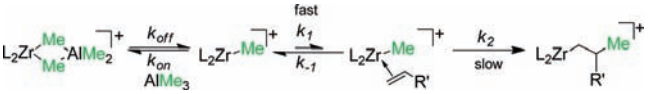

CONCLUSIONS

The kinetics we have observed for carboalumination (reaction 4) strongly support the mechanism in Scheme 1, and our data on Zr-catalyzed chain growth (reaction 5) are consistent with the analogous mechanism in Scheme 3. The coordination of AlR_3 to the catalytically active organozirconium cation (**B**) is a preequilibrium that lies toward the $(\mu\text{-}R)_2$ heterobimetallic (**A**) under reaction conditions but is rapidly maintained on the time scale of the overall reaction. However, actual transfer of the growing chains appears to be somewhat slow, which may reflect a strong preference for bridging methyls over longer chain bridging alkyl groups.

The fact that no [olefin] term is observed in the denominator of either rate law (i.e., that eq 13 reduces to eq 14, and eq 20 to eq 21) implies that the concentration of the olefin complex **C** is negligible compared to that of the heterobimetallic **A** or the cation **B**. Two explanations are possible: either insertion is fast relative to the coordination of the olefin (Scheme 6) or the olefin is bound in a rapid but unfavorable equilibrium before rate-determining insertion (Scheme 7). There is experimental support for Scheme 7 in the case of incoming alkynes[39] and 1-alkenes.[40] With incoming ethylene, chain growth is too fast to permit rate measurements and is usually diffusion controlled.

The relative efficiency of various Zr complexes as catalysts may be a function of k_1 (if Scheme 6 is correct) or k_1k_2/k_{-1} (if Scheme 7 is correct). However, a major factor—likely to be dominant in many cases—will be the size of the equilibrium constant K for the dissociation of the corresponding Zr/Al heterobimetallic.

EXPERIMENTAL SECTION

General Considerations. An inert atmosphere and Schlenk line methods were used to handle air and moisture sensitive compounds. Benzene was distilled from sodium/benzophenone under N_2 prior to use. Diethyl ether and toluene were purified using a standard Grubbs-type solvent system. Hexanes were first deolefinated by stirring with H_2SO_4, then dried over sodium, distilled, and stored under argon. Stock solutions were made inside a glovebox and stored in a −20 °C freezer when not in use.

Synthesis of (EBI)ZrMe$_2$. MeMgBr (1.7 mL, 3 M in hexanes) was added to ~50 mL of diethylether in a Schlenk flask under nitrogen. Dioxane (0.5 mL) was then added, generating $MgMe_2$ and $MgBr_2$ (immediate white precipitate). After stirring for ~1 h, the solids were allowed to settle and the solution was transferred by filter cannula to

another Schlenk flask containing *rac*-(EBI)$ZrCl_2$ (0.75 g, 1.56 mmol) slurried in ~50 mL of diethyl ether at −78 °C. The reaction was allowed to warm to room temperature overnight. The solvent was then removed, leaving a yellow solid. This solid was dissolved in benzene, resulting in a yellow solution and a white solid ($MgCl_2$). The solution was then filtered and the solvent removed under vacuum, leaving 620 mg (91% yield) of a pure yellow solid. The product may be recrystallized from toluene/hexanes. ^{1}H NMR (500 MHz, C_6D_6): δ 7.31 (d, C_6H, J_{H-H} = 8.5 Hz, 2H), 7.06 (m, C_6H, 4H), 6.89 (m, C_6H, 2H), 6.41 (d, C_5H, J_{H-H} = 3.3 Hz, 2H), 5.65 (d, C_5H, J_{H-H} = 3.3 Hz, 2H), 2.83−2.66 (m, CH_2CH_2, 4H), −0.97 (s, ZrMe_2, 6H).

Synthesis of Cp_2ZrMe_2.[41] Cp_2ZrCl_2 (3.0 g, 10.26 mmol) was added to a Schlenk flask with a stir bar. Dry Et_2O (150 mL) was added by cannula to the flask. The flask was cooled to −78 °C, and 19.25 mL of 1.6 M LiMe/MgBr (30.78 mmol) were added slowly by syringe with stirring. The reaction was allowed to warm to room temperature over the course of 3 h. Chlorotrimethylsilane (1.3 mL, 10.26 mmol) was then added by syringe, and the reaction was stirred for 1 h. The volatiles were removed under vacuum. The product was extracted away from the lithium salts by the addition of 50 mL of benzene followed by cannula filtration. The benzene was removed under vacuum, leaving 2.21 g of white solid (86%). ^{1}H NMR (500 MHz, C_6D_6): δ 5.72 ppm (s, C_5H_5, 10H), −0.129 ppm (s, CH_3, 6H).

Synthesis of $Me_2C(Cp)_2ZrMe_2$. The same procedure for the preparation of Cp_2ZrMe_2 was followed with the substitution of $Me_2C(Cp)_2ZrCl_2$ for Cp_2ZrCl_2. The reaction was scaled down to 300 mg (0.9 mmol) of $Me_2C(Cp)_2ZrCl_2$ starting material and yielded 190 mg of product (72%). ^{1}H NMR (500 MHz, C_6D_6): δ 6.33 ppm (d, J_{H-H} = 3.0 Hz, C_5H, 4H), 5.11 ppm (d, J_{H-H} = 3.0 Hz, C_5H, 4H), 1.12 ppm (s, CCH_3, 6H), 0.03 ppm (s, $ZrCH_3$, 6H).

General Procedure for Kinetic Studies of Carboalumination. A stock solution of activated catalyst was prepared in the glovebox by adding (EBI)$ZrMe_2$ (18.9 mg, 0.05 mmol) to $[Ph_3C][B(C_6F_5)_4]$ (46.1 mg, 0.05 mmol) and 10 mL of C_6D_6 in an amber vial wrapped in aluminum foil. The solution was allowed to sit overnight. Trimethylaluminum (10 μL, 0.11 mmol) was added, and the solution was allowed to react for 1 h. The solution was then filtered through glass wool into a new vial, and the concentration catalyst was determined by ^{1}H NMR against a toluene internal standard. Typical concentrations of catalyst stock solutions were 1−2 mM. A C_6D_6 stock solution that was 61.2 mM in allylbenzene and 61.2 mM in toluene and a 612 mM (in Al) stock solution of $AlMe_3$ in C_6D_6 were prepared.

For each run, the probe temperature was set to 40 °C and calibrated with an ethylene glycol standard. Each set of conditions was repeated for a total of three consistent trials. Samples were prepared at the same time and frozen until use. Reactions were monitored by ^{1}H NMR at 500 MHz. Three scans were taken every 120 s with a 3 s acquisition time and 1 s delay, making the time between points 132 s. Integration of the allylbenzene vinylic peaks (5.05−5.10 ppm) versus the toluene methyl group as a standard was used for the fitting procedure. The data were imported into Kaleidagraph and fit to a two-parameter first-order decaying exponential.

Dependence on Catalyst. Samples were all 500 μL total volume. To a J. Young tube containing 50 μL of $AlMe_3$ solution was added the desired amount of catalyst solution. Enough C_6D_6 to give a total volume of 450 μL was then added, and the tube was frozen in a −20 °C freezer. Once frozen, 50 μL of allylbenzene solution were added. The tube was resealed and then frozen until use. Catalyst concentrations tested were 0.275, 0.455, and 0.691 mM.

Dependence on $AlMe_3$. Samples were prepared exactly as above except for the following. The total reaction volume was 600 μL, $AlMe_3$ was varied, 25 μL of allylbenzene solution were used, and the catalyst loading was 15% with respect to allylbenzene for each run. Enough trimethylaluminum was added to produce solutions 18.4, 36.7, 73.4, 91.8, and 275 mM in Al—which were respectively 0.46, 0.65, 0.93, 1.04, and 1.8 mM in monomeric $AlMe_3$.

Inhibition Kinetics of $[Cp_2Zr(\mu\text{-}Me)_2AlMe_2^+][B(C_6F_5)_4^-]$ and $[Me_2C(Cp)_2Zr(\mu\text{-}Me)_2AlMe_2^+][B(C_6F_5)_4^-]$. The procedure for dependence on $AlMe_3$ was followed as above except that 12.6 mg of Cp_2ZrMe_2 or 14.6 mg of $Me_2C(Cp)_2ZrMe_2$ were substituted for 18.9 mg of *rac*-(EBI)$ZrMe_2$. For these catalysts it was necessary to add ~5 equiv of $AlMe_3$ to the activated species $[L_2ZrMe^+][B(C_6F_5)_4^-]$ to quantitatively form the corresponding Zr/Al heterobimetallic.

Stoichiometric Reaction of $[Cp_2Zr(\mu\text{-}Me)_2AlMe_2^+][B(C_6F_5)_4^-]$ with $AlMe_3$. A stock solution of activated catalyst was prepared in the glovebox by adding Cp_2ZrMe_2 (12.6 mg, 0.04 mmol) to $[Ph_3C][B(C_6F_5)_4]$ (46.1 mg, 0.04 mmol) and ~10 mL of C_6D_6 in an amber vial wrapped in aluminum foil. The solution was allowed to sit overnight. The solution was then filtered through glass wool into another amber vial. Into a J. Young tube was transferred 0.5 mL of the solution and 0.100 mL of 9.388 mM toluene in C_6D_6 as an internal standard. A ^{1}H NMR spectrum was acquired at 40 °C with a delay time of 12 s to ensure accurate integrations of all peaks (the T_1 of the toluene methyl resonance is 2.3 s under these conditions). The concentration of the zirconium methyl cation was calculated against the toluene standard. Meanwhile, 5 μL of neat $AlMe_3$ was diluted to 5 mL in C_6D_6 to yield a 0.0104 M solution. The appropriate quantity of this solution was then added to the J-Young tube containing the zirconium methyl cation. After allowing the tube to equilibrate to the 40 °C probe temperature, another ^{1}H NMR spectrum was acquired. Representative spectra can be found in Figures S6−S8.

General Procedure for Kinetic Studies of Chain Growth. A stock solution of activated catalyst was prepared in the glovebox as described for carboalumination.

The flow controller and flow meter were turned on at least 30 min prior to use to allow the instruments to warm up and equilibrate. Inside a glovebox, the desired amounts of catalyst and $AlMe_3$ were added to enough toluene to make a 100 mL solution. The solution was added to the pressure reaction vessel, and the vessel was closed inside the glovebox, removed, and placed in the recirculating cold bath to cool. During this time it was connected to the manifold, thermocouple meter, mechanical stirrer, and ethylene feed. The mechanical stirrer was set to a 75% maximum stir rate. The reactor was evacuated and backfilled with argon twice and then evacuated a final time before the reaction began.

Before opening the ethylene valve, the desired pressure was set on the regulator and the flow controller was fully open for initial pressurization. The reaction was started by opening the ethylene feed. ***Caution:*** *Always shield pressurized vessels!* When the flow meter showed that the rate of ethylene uptake was below 300 SCC (the maximum of accurate measurement), the flow controller was switched from fully open to the "controlled" position, allowing accurate measurement of flow. The reaction was allowed to proceed for 5 min, and then the stir rate was increased to maximum for an additional minute. Typically, the reactor was completely pressurized after 1.5 min of total elapsed time. Reactions were quenched by injection of 3.0 mL of triethylamine.

Pressure Dependence. Reactions were carried out with 4.2 mL of $AlMe_3$ (0.439 M in Al) and 4.39×10^{-6} M [*rac*-(EBI)$Zr(\mu\text{-}Me)_2AlMe_2^+][B(C_6F_5)_4^-]$. The pressures tested were 20, 30, and 40 psig.

Catalyst Dependence. Reactions were carried out with 4.2 mL of $AlMe_3$ (0.439 M in Al) and 20 psig of ethylene pressure. The concentrations of [*rac*-(EBI)$Zr(\mu\text{-}Me)_2AlMe_2^+][B(C_6F_5)_4^-]$ catalyst tested were 8.78×10^{-6}, 4.39×10^{-6}, 2.195×10^{-6}, and 1.098×10^{-6} M.

AlR_3 Dependence. Reactions were carried out under 20 psig of ethylene pressure with 4.39×10^{-6} M [*rac*-(EBI)$Zr(\mu\text{-}Me)_2AlMe_2^+][B(C_6F_5)_4^-]$. Enough trimethylaluminum was added to produce solutions 0.439, 0.220, 0.110, 0.055, and 0.329 M in Al.

Hydrolysis (and Oxidation) of Aluminum Alkyls from Chain Growth Experiments. The reaction mixture was quenched by injection of 3 mL of triethylamine into the reactor. The solution was then poured slowly into 500 mL of acidified (with HCl) methanol.

Additional HCl was added until all aluminum salts were dissolved, leaving the precipitated polymer. The polymer was collected by suction filtration and dried for 24 h at 60 °C in a vacuum oven. The resulting polymer was then analyzed by GPC and ^{1}H and ^{13}C NMR (see spectra in the Supporting Information). For samples that required oxidation, dry O_2 was bubbled through the reaction solution for 8 h after quenching. Precipitation of the resulting products was performed as above.

Controlled Flow Chain Growth Reaction. A chain growth reaction (20 psig ethylene, 4.39×10^{-6} M [*rac*-(EBI)Zr(μ-Me)$_2$-AlMe$_2^+$][B(C$_6$F$_5$)$_4^-$], 0.439 M in Al) was performed with the following changes to the general procedure. First, the mass flow controller was allowed to restrict the flow of ethylene to no more than 300 SCC/min over the entire course of the reaction. Second, the reaction time was extended to 8 min to ensure saturation before rate measurement. Third, hydrolysis of the quenched product mixture was carried out by pouring it into 300 mL of 20% HCl (aq) with vigorous stirring. Polymeric product (106 mg) immediately precipitated and was collected by filtering the biphasic solution. The organic layer of the filtrate was then separated, and the aqueous layer washed with toluene (2×25 mL). The combined organic layers were washed with 1.0 M $NaHCO_3$ (aq) and dried over Na_2SO_4. The rate of the reaction was determined to be 0.143 SCC/min, in excellent agreement with the rates determined from other experiments at these concentrations (see Supporting Information). ^{1}H NMR analysis of the toluene solution of the product indicated the presence of oligomeric materials (Figure S-11). ^{1}H NMR (400 MHz, $CDCl_3$): δ 1.16 (m, $CH_3(CH_2)_6CH_3$, 13H), 0.87 (m, $CH_3(CH_2)_6CH_3$, 1H). MALDI-TOF and FD-MS analyses of these oligomeric minor products were inconclusive. The polymer was analyzed by GPC and found to have M_n = 67 500, M_w= 172 500, PDI = 2.56 (Figure S-12). ^{1}H NMR analysis of the polymer (Figure S-13) showed very little detectable unsaturation.

Chain Growth Using Al(oct)$_3$. The reaction was carried out as described in the general procedures with 4.39×10^{-6} M [*rac*-(EBI)-Zr(μ-Me)$_2$AlMe$_2^+$][B(C$_6$F$_5$)$_4^-$], 20 psig ethylene, 0.439 M in Al. Ethylene uptake plots deviated slightly from linearity after ethylene saturation. The rate estimated from the ethylene-saturated region was about 0.18 SCC/s. Hydrolysis of the resulting quenched product mixture was carried out by pouring the reaction mixture into 300 mL of 20% HCl (aq) with vigorous stirring. Polymeric product (176 mg) immediately precipitated and was collected by filtering the biphasic solution. The organic layer of the filtrate was then separated, and the aqueous layer washed with toluene (2×25 mL). The combined organic layers were washed with 1.0 M $NaHCO_3$ (aq) and dried over Na_2SO_4. ^{1}H NMR analysis of the toluene solution of product indicated only the presence of octane (Figure S-14). ^{1}H NMR (400 MHz, $CDCl_3$): δ 1.26 (b, $CH_3(CH_2)_6CH_3$, 13H), 0.88 (t, $CH_3(CH_2)_6CH_3$, J_{H-H} = 5.4 Hz, 1H). GPC of the resuting polymer (Figure S-15) showed it to have M_w = 127 500, M_n = 56 000, and PDI = 2.26. ^{1}H NMR of the polymer (Figure S-16) showed it to have a small but detectable amount of vinyl content.

■ ASSOCIATED CONTENT

Supporting Information. Tables S-1 through S-5, Figures S-1 through S-16, derivation of the rate law for an alternative mechanism for carboalumination, and details of the polymer reactor design are available. This material is available free of charge via the Internet at http://pubs.acs.org.

■ AUTHOR INFORMATION

Corresponding Author
jrn11@columbia.edu

■ ACKNOWLEDGMENT

We are grateful to Bryan Coughlin for advice on the design of the equipment in Figure 5, to Exxon for the molecular weight determinations, to Boulder Scientific for compounds, and to the National Science Foundation (CHE 0749537) for support. We thank Condea Vista (now SASOL) for support of the initial phase of this investigation. We also thank A. K. Rappe, Frank Rix, and Clark Landis for helpful discussions.

■ REFERENCES

(1) Fallis, A. G.; Forgione, P. *Tetrahedron* **2001**, *57*, 5899–5913.
(2) (a) Mason, M. R.; Song, B.; Kirschbaum, K. *J. Am. Chem. Soc.* **2004**, *126*, 11812–11813. (b) Lehmkuhl, H. *Angew. Chem.* **1964**, *76*, 817. (c) Rowley, C. N.; DiLabio, G. A.; Barry, S. T. *Inorg. Chem.* **2005**, *44*, 1983–1991. (d) Chang, C. C.; Hsiung, C. S.; Su, H. L.; Srinivas, B.; Chiang, M. Y.; Lee, G. H.; Wang, Y. *Organometallics* **1998**, *17*, 1595–1601.
(3) Dzhemilev, U. M.; Ibragimov, A. G.; Vostrikova, O. S.; Tolstikov, G. A. *Bull. Acad. Sci. USSR, Div. Chem. Sci.* **1985**, *34*, 196–197.
(4) (a) Erker, G. *Pure Appl. Chem.* **1992**, *64*, 393–401. (b) Erker, G.; Aulbach, M.; Knickmeier, M.; Wingbermuhle, D.; Kruger, C.; Nolte, M.; Werner, S. *J. Am. Chem. Soc.* **1993**, *115*, 4590–4601.
(5) (a) Negishi, E.-I.; Kondakov, D. Y. *Chem. Soc. Rev.* **1996**, *25*, 417–426. (b) Negishi, E. *Pure Appl. Chem.* **2001**, *73*, 239–242. (c) Negishi, E.-I.; Huo, S. Q. *Pure Appl. Chem.* **2002**, *74*, 151–157. (d) Negishi, E., Tan, Z. *Topics in Organometallic Chemistry*; Springer: Berlin, Heidelberg, 2004; Vol. 8, pp 139−176. (e) Negishi, E.-I. *Dalton Trans.* **2005**, 827–848.
(6) Noweck, K. *Ullmann's Encyclopediaof Industrial Chemistry*, 7th ed.; Wiley-VCH Verlag GmbH & Co. KGaA: Weinheim, 2006.
(7) Samsel, E. G. Catalyzed Chain Growth Process. Patent US5210338.
(8) Samsel, E. G.; Eisenberg, D. C. Chain growth reactions of α-olefin(s) - by chain growth on an aluminium alkyl using a activated actinide metallocene, useful for production of linear olefin(s) and alcohol (s). Patent US5276220.
(9) Bazan, G. C.; Rogers, J. S.; Fang, C. C. *Organometallics* **2001**, *20*, 2059–2064.
(10) (a) Ganesan, M.; Gabbai, F. P. *Organometallics* **2004**, *23*, 4608–4613. (b) Mani, G.; Gabbai, F. P. *Angew. Chem., Int. Ed.* **2004**, *43*, 2263–2266. (c) Ganesan, M.; P. Gabbai, F. *J. Organomet. Chem.* **2005**, *690*, 5145–5149.
(11) Rouholahnejad, F.; Mathis, D.; Chen, P. *Organometallics* **2010**, *29*, 294–302.
(12) (a) Kretschmer, W. P.; Meetsma, A.; Hessen, B.; Schmalz, T.; Qayyum, S.; Kempe, R. *Chem.—Eur. J.* **2006**, *12*, 8969–8978. (b) Kretschmer, W. P.; Bauer, T.; Hessen, B.; Kempe, R. *Dalton Trans.* **2010**, *39*, 6847–6852.
(13) (a) Britovsek, G. J. P.; Cohen, S. A.; Gibson, V. C.; van Meurs, M. *J. Am. Chem. Soc.* **2004**, *126*, 10701–10712. (b) van Meurs, M.; Britovsek, G. J. P.; Gibson, V. C.; Cohen, S. A. *J. Am. Chem. Soc.* **2005**, *127*, 9913–9923.
(14) (a) Arriola, D. J.; Carnahan, E. M.; Hustad, P. D.; Kuhlman, R. L.; Wenzel, T. T. *Science* **2006**, *312*, 714–719. (b) Kuhlman, R. L.; Wenzel, T. T. *Macromolecules* **2008**, *41*, 4090–4094. (c) Hustad, P. D.; Kuhlman, R. L.; Carnahan, E. M.; Wenzel, T. T.; Arriola, D. J. *Macromolecules* **2008**, *41*, 4081–4089. (d) Hustad, P. D.; Kuhlman, R. L.; Arriola, D. J.; Carnahan, E. M.; Wenzel, T. T. *Macromolecules* **2007**, *40*, 7061–7064. (e) Wenzel, T. T.; Arriola, D. J.; Carnahan, E. M.; Hustad, P. D.; Kuhlman, R. L. In *Topics in Organometallic Chemistry*; Guan, Z., Ed.; Springer: Berlin, 2009; Vol. 26, pp 65−104.
(15) (a) Wei, J.; Zhang, W.; Sita, L. *Angew. Chem., Int. Ed.* **2010**, *49*, 1768–1772. (b) Sita, L. R. *Angew. Chem., Int. Ed.* **2009**, *48*, 2464–2472. (c) Zhang, W.; Sita, L. R. *J. Am. Chem. Soc.* **2008**, *130*, 442−443. (d) Zhang, W.; Wei, J.; Sita, L. R. *Macromolecules* **2008**, *41*, 7829–7833.
(16) (a) Bochmann, M.; Lancaster, S. J. *J. Organomet. Chem.* **1995**, *497*, 55–59. (b) Bochmann, M.; Lancaster, S. J. *Angew. Chem., Int. Ed.* **1994**, *33*, 1634–1637.

(17) Petros, R. A.; Norton, J. R. *Organometallics* **2004**, *23*, 5105–5107.

(18) (a) Lieber, S.; Brintzinger, H. H. *Macromolecules* **2000**, *33*, 9192–9199. (b) Pedeutour, J.-N.; Radhakrishnan, K.; Cramail, H.; Deffieux, A. *Macromol. Rapid Commun.* **2001**, *22*, 1095–1123. (c) Pedeutour, J.-N.; Radhakrishnan, K.; Cramail, H.; Deffieux, A. *J. Mol. Catal. A: Chem.* **2002**, *185*, 119–125. (d) Götz, C.; Rau, A.; Luft, G. *Macromol. Mater. Eng.* **2002**, *287*, 16–22. (e) Götz, C.; Rau, A.; Luft, G. *J. Mol. Catal. A: Chem.* **2002**, *184*, 95–110. (f) Götz, C.; Rau, A.; Luft, G. *Macromol. Symp.* **2002**, *178*, 93–107. (g) Bryliakov, K. P.; Semikolenova, N. V.; Yudaev, D. V.; Zakharov, V. A.; Brintzinger, H.-H.; Ystenes, M.; Rytter, E.; Talsi, E. P. *J. Organomet. Chem.* **2003**, *683*, 92–102. (h) Kempe, R. *Chem.—Eur. J.* **2007**, *13*, 2764–2773. (i) Bochmann, M. *Organometallics* **2010**, *29*, 4711–4740.

(19) Bolton, P. D.; Clot, E.; Cowley, A. R.; Mountford, P. *J. Am. Chem. Soc.* **2006**, *128*, 15005–15018.

(20) Shaughnessy, K. H.; Waymouth, R. M. *Organometallics* **1998**, *17*, 5728–5745.

(21) Lee, C. H.; Lee, S. J.; Park, J. W.; Kim, K. H.; Lee, B. Y.; Oh, J. S. *J. Mol. Catal. A: Chem.* **1998**, *132*, 231–239.

(22) Chen, E. Y.-X.; Marks, T. J. *Chem. Rev.* **2000**, *100*, 1391–1434.

(23) (a) Song, F. Q.; Cannon, R. D.; Lancaster, S. J.; Bochmann, M. *J. Mol. Catal. A: Chem.* **2004**, *218*, 21–28. (b) Chien, J. C. W.; Tsai, W. M.; Rausch, M. D. *J. Am. Chem. Soc.* **1991**, *113*, 8570–8571. (c) Chen, E. Y.-X.; Marks, T. J. *Chem. Rev.* **2000**, *100*, 1391–1434.

(24) Petros, R. A.; Camara, J. M.; Norton, J. R. *J. Organomet. Chem.* **2007**, *692*, 4768–4773.

(25) Excess $AlMe_3$ was added so that the heterobimetallic **3** was the only Zr species observable in the solution ^1H NMR. Typically, 5−10 mL were sufficient.

(26) Cerny, Z.; Fusek, J.; Kriz, O.; Hermanek, S.; Solc, M.; Casensky, B. *J. Organomet. Chem.* **1990**, *386*, 157–165.

(27) Bochman and Lancaster (ref 16) have said that alkylaluminum adducts like **3** "are coordinatively saturated and lack a vacant orbital suitable for binding the olefinic substrate". While their coordinative saturation can be questioned (note the vacant nonbonding orbital in Figure 4 of ref 19), there seems to be general agreement on their inability to bind olefins.

(28) Cornish-Bowden, A. *Fundamentals of enzyme kinetics*; Brookfield: Portland, London, 1995.

(29) The standard deviations given for each value of K take into account the covariance between the least-squares intercept and the least-squares slope.

(30) The uncertainties given in Table 1 result from a generous estimate (A. D. Bain, McMaster, 2003) of the covariance of k_{off} with other parameters fitted by CiFIT (ref 31). The uncertainties previously reported (ref 17) came directly from CiFIT and did not include covariance.

(31) Bain, A. D.; Cramer, J. A. *J. Magn. Reson.* **1996**, *118*, 21–27.

(32) (a) Konobeev, B. I.; Lyapin, V. V. *Khimicheskaya Promyshlennost (Moscow, Russian Federation)* **1967**, *43*, 114–16. (b) Jolley, J. E.; Hildebrand, J. H. *J. Am. Chem. Soc.* **1958**, *80*, 1050–1054. (c) Coan, C. R.; King, A. D. *J. Chromatogr.* **1969**, *44*, 429–436.

(33) (a) Smith, M. B. *J. Organomet. Chem.* **1970**, *22*, 273–281. (b) Smith, M. B. *J. Organomet. Chem.* **1972**, *46*, 31–49. (c) Smith, M. B. *J. Organomet. Chem.* **1972**, *46*, 211–217. (d) Smith, M. B. *J. Organomet. Chem.* **1974**, *70*, 13–33. (e) Smith, M. B. *J. Phys. Chem.* **1967**, *71*, 364–370.

(34) The flow controller and flow meter are only accurate at flow rates below 300 SCC/min.

(35) Talsi, E. P.; Eilertsen, J. L.; Ystenes, M.; Rytter, E. *J. Organomet. Chem.* **2003**, *677*, 10–14.

(36) Two small additional signals, at −0.24 and −0.57 (ratio approximately 2:1), appear when Me_3Al is first added to $[Cp_2ZrMe][B(C_6F_5)_4]$; they disappear when the $AlMe_3$ exceeds 1 equiv. Their assignment (perhaps a 2:1 Zr/Al adduct?) is unclear.

(37) Segel, I. H. *Enzyme kinetics: behavior and analysis of rapid equilibrium and steady state enzyme systems*; Wiley: New York, 1975.

(38) Partial noncompetitive inhibition can be distinguished kinetically from competitive inhibition by increasing the concentration of inhibitor. This is impractical in our system due to the unfavorable monomer/dimer equilibrium of $AlMe_3$.

(39) Sydora, O. L.; Kilyanek, S. M.; Jordan, R. F. *J. Am. Chem. Soc.* **2007**, *129*, 12952−12953.

(40) (a) Landis, C. R.; Rosaaen, K. A.; Uddin, J. *J. Am. Chem. Soc.* **2002**, *124*, 12062–12063. (b) Dahlmann, M.; Erker, G.; Bergander, K. *J. Am. Chem. Soc.* **2000**, *122*, 7986–7998.

(41) (a) Gately, D. A.; Norton, J. R.; Goodson, P. A. *J. Am. Chem. Soc.* **1995**, *117*, 986–996. (b) Grossman, R. B. Ph.D. Thesis, Massachusets Institute of Technology, 1992.